ACS APPLIED MATERIALS & INTERFACES

Letter

www.acsami.org

# Raspberrylike $SiO_2$@Reduced Graphene Oxide@AgNP Composite Microspheres with High Aqueous Dispersity and Excellent Catalytic Activity

Wei Xiao,* Yanhua Zhang,* and Bitao Liu

Research Institute for New Materials Technology, Chongqing University of Arts and Sciences, Yongchuan Chongqing 402160, China

Supporting Information

**ABSTRACT:** The hybridizations of functional microspheres with graphene or graphene oxide (GO) sheets often suffer from severe agglomeration behaviors, leading to poor water dispersity of the resultant composite materials. Here, we first demonstrate that the sonication-assisted self-assembly of tiny GO sheets (whose lateral size less than 200 nm) on microspheric substrates like cationic polyelectrolyte-modified $SiO_2$ microspheres could effectively overcome such a common drawback. On the basis of this facile strategy, we further developed reduced graphene oxide/silver nanoparticle composite film wrapped $SiO_2$ microspheres, which not only possessed unique raspberrylike structure and high aqueous dispersity but also exhibited exceptional catalytic activity toward the reduction of 4-nitrophenol.

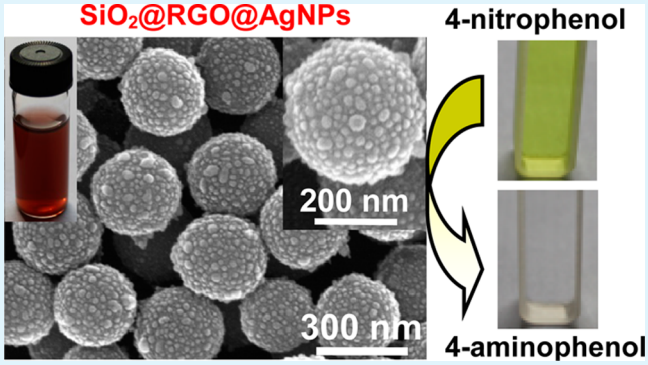


**KEYWORDS:** *graphene, microspheres, silver nanoparticles, sonication-assisted self-assembly, catalytic reduction*

Since its discovery, graphene, a single-atom-thick planar sheet of graphite, has emerged as a promising nanomaterial because of its unique two-dimensional honeycomb structure and remarkable physicochemical properties, such as splendid charge mobility, high thermal conductivity, great mechanical strength, and huge surface area.[1,2] As a consequence, various graphene-based composite materials have been extensively explored and applied to lots of important fields like catalysis, sensing, energy storage, drug delivery, and so on.[3−7] However, most of them were generally fabricated by introducing diverse nanoparticles (including noble metal, metal oxide, metal sulfide, and polymer nanoparticles) onto the surface of graphene oxide (GO) sheets, followed by the reduction of GO component to reduced graphene oxide (RGO).[3−7] In this manner, GO sheets were utilized as supports and the functional nanoparticles were deposited or grown as guest substances, resulting in unitarily structural and morphological characteristics of the final RGO/nanoparticle composite materials.[8] By contrast, reports regarding the self-assembly of GO or RGO sheets onto a certain scaffold to synthesize GO- and RGO-based composite materials are relatively limited. Recently, a series of GO- and RGO-based multilayer films as well as paper-like GO- and RGO-based composite materials have been commendably prepared based on self-assembly of GO or RGO sheets onto bulk solid supports like glass plate, plastic slice and silicon wafer.[9−12] Obviously, these substrates used for depositing GO and RGO sheets are flat and smooth, which are not beneficial for constructing morphologically complicated GO- and RGO-based composite materials. Therefore, to acquire high-performance GO- and RGO-based composite materials with unique structures, self-assembly of GO or RGO sheets at nonplanar interfaces seems to be a facile and feasible choice. Previously, by mixing aqueous suspensions of GO sheets with those of surface-aminated $TiO_2$, CdS and $Co_3O_4$ microspheres respectively, these microspheric substances were wrapped with GO sheets, leading to the formation of $TiO_2$/GO, CdS/GO, and $Co_3O_4$/GO composite microspheres, which were successively converted into $TiO_2$/RGO, CdS/RGO and $Co_3O_4$/RGO composite microspheres after hydrothermal or chemical reduction of the outer GO component to RGO.[13−15] In a similar way, positively charged polymer microspheres were also modified with negatively charged GO and RGO sheets through electrostatic interaction, thus achieving the preparation of polymer/GO and polymer/RGO composite microspheres.[16,17] Unfortunately, the GO or RGO suspensions adopted in these systems contained plenty of large GO or RGO sheets with lateral size exceeding a few micrometers. That means the area of a single large GO or RGO sheet is much greater than that of one microsphere, and an individual micrometer-sized GO or RGO sheet is able to capture many microspheres. As a result, the synthesized GO- and RGO-containing composite microspheres were linked together by GO and RGO sheets, respectively, bringing about serious

Received: January 11, 2015
Accepted: March 9, 2015
Published: March 9, 2015





DOI: 10.1021/acsami.5b00296
ACS Appl. Mater. Interfaces 2015, 7, 6041−6046

aggregation phenomena.[18−22] It is assumed that such poor dispersity may be harmful to their further functionalization and severely restricted their application potential. Hence, how to overcome the agglomeration behaviors during the hybridization process of GO or RGO sheets with the nonplanar substrates and how to promote the dispersity of the resultant GO- and RGO-based composite materials remain to be solved.

As we know, sonication is a useful tool for dispersing samples and preventing aggregation, and according to the above analysis, narrowing the lateral sizes of GO and RGO sheets is also likely to ease the degree of aggregation behaviors during their self-assembly process. Consequently, assembling small GO or RGO sheets on nonplanar supports with the aid of intense sonication would effectively circumvent aggregation phenomena and enable us to obtain highly water-dispersible GO- and RGO-based composite materials with distinct morphologies and properties. Inspired by this idea, herein, sonication-assisted self-assembly of tiny GO sheets (whose lateral size less than 200 nm) on microspheric substrates like cationic polyelectrolyte-modified $SiO_2$ microspheres was first realized, yielding uniform GO thin layer coated $SiO_2$ microspheres (Figure 1), which were exempted from the cross-

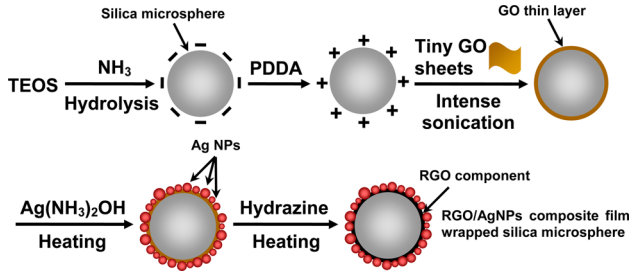


**Figure 1.** Schematic illustration of the fabrication of RGO/AgNP film wrapped $SiO_2$ microspheres.

linking by GO sheets and thus possessed outstanding aqueous dispersity. By in situ synthesis of silver nanoparticles (AgNPs) on such GO wrapped $SiO_2$ microspheres, followed by chemical reduction of the incorporated GO component to RGO, raspberrylike RGO/AgNP film wrapped $SiO_2$ microspheres were further developed (Figure 1), which featured excellent water dispersity as well and rendered exceptional catalytic activity toward the reduction reaction of 4-nitrophenol by $NaBH_4$.

The monodisperse $SiO_2$ microspheres with diameter of ∼280 nm (Figure 2a and Figure S1 in the Supporting Information) were synthesized by hydrolyzing tetraethyl orthosilicate (TEOS) in an alcoholic medium in the presence of water and ammonia employing a modified Stöber method (see the Supporting Information for experimental details).[18,19] The as-prepared $SiO_2$ microspheres were negatively charged with the zeta potential of −46.5 mV, and they were subsequently positively charged with a cationic polyelectrolyte poly(diallyldimethylammonium) chloride (PDDA) (see the Supporting Information for experimental details). The zeta potentials of the resultant PDDA-modified $SiO_2$ microspheres and the tiny GO sheets (whose lateral sizes less than 200 nm) (Figure S2a,b in the Supporting Information) were 22.4 mV and −45.1 mV, respectively, suggesting that they were oppositely charged. Therefore, the tiny GO sheets were capable of self-assembling on the surface of the PDDA-modified $SiO_2$ microspheres through electrostatic interaction under violent

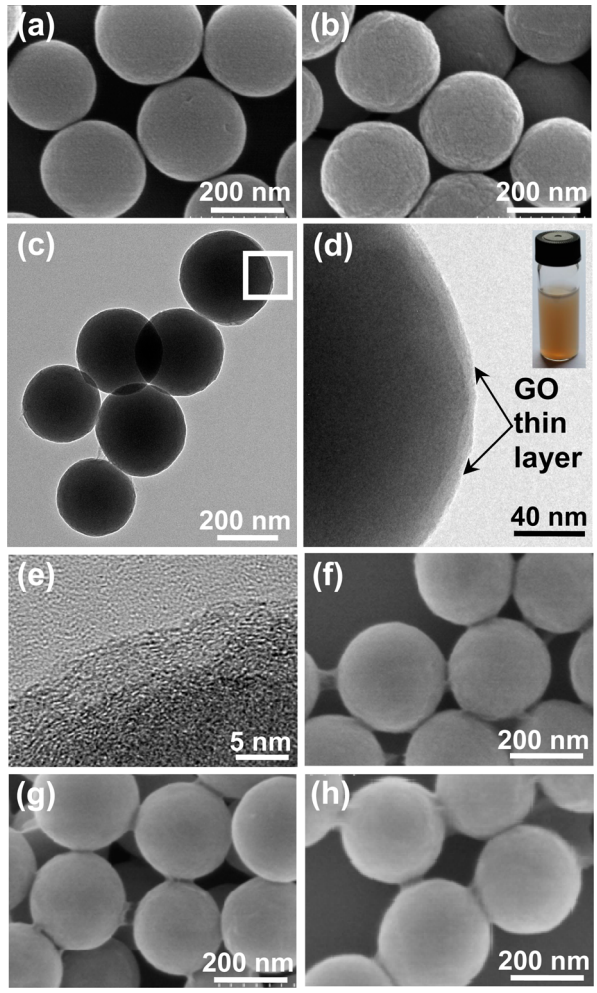


**Figure 2.** (a) Scanning electron microscopy (SEM) image of pure $SiO_2$ microspheres, showing smooth surface. (b) SEM image of GO wrapped $SiO_2$ microspheres (i.e., $SiO_2$@GO composite microspheres), displaying relative rough surface. (c) Transmission electron microscopy (TEM) image of $SiO_2$@GO composite microspheres. (d) TEM image of the morphological details of the boxed area in (c); the inset is the photograph of an aqueous suspension of $SiO_2$@GO composite microspheres after standing overnight, demonstrating the excellent water dispersity. (e) Representative high-resolution TEM (HRTEM) image of a $SiO_2$@GO composite microsphere. (f−h) SEM images of GO wrapped $SiO_2$ microspheres synthesized using tiny GO sheets under vigorous stirring, using tiny GO sheets under low-intensity sonication (50 W), and using micrometer-sized GO sheets under intense sonication (160 W), respectively.

sonication (160 W) (see the Supporting Information for experimental details).[15] As envisioned, the surface charge of the resultant composite microspheres was negative with the zeta potential of −43.8 mV, indicating the formation of GO wrapped $SiO_2$ microspheres (denoted as $SiO_2$@GO). It is noted that the GO and RGO components incorporated in the currently developed composite microspheres are derived from the tiny GO sheets unless otherwise specified. The sonication-assisted self-assembly process is very rapid so that it could be completed within 20 min and the content of the GO component deposited on $SiO_2$@GO composite microspheres is 1.45% by weight as revealed by UV−vis spectroscopy (Figure S3 in the Supporting Information).

Figure 2b and Figure S4 in the Supporting Information show SEM images of the $SiO_2$@GO composite microspheres, whose


DOI: 10.1021/acsami.5b00296
ACS Appl. Mater. Interfaces 2015, 7, 6041−6046

sizes are almost the same as those of pure $SiO_2$ microspheres. Nevertheless, compared with the smooth spherical surface of $SiO_2$ microspheres (Figure 2a), a little external surface roughness is observed for the $SiO_2$@GO composite microspheres (Figure 2b), which should be ascribed to the deposition of tiny GO sheets on their surface. Careful TEM examinations of the $SiO_2$@GO composite microspheres were also conducted. As can be clearly seen in Figure 2c−e, a uniform thin layer with thickness of ∼6 nm is seamlessly coated on a microspheric substrate, further demonstrating the successful self-assembly of tiny GO sheets on $SiO_2$ microspheres. Unlike the previously reported GO-wrapped microspheres, which were short of enough water dispersity,[13−17] the dried $SiO_2$@GO composite microspheres were easily redispersed in water, and the resultant brown suspension remained rather homogeneous even after standing overnight (inset of Figure 2d). Undoubtedly, such superior aqueous dispersity of $SiO_2$@GO composite microspheres should be attributed to freeing from cross-linking by GO sheets as verified by SEM and TEM inspections (Figure 2b, c and Figure S4 in the Supporting Information). As control, the hybridizations of tiny GO sheets with PDDA-modified $SiO_2$ microspheres under vigorous stirring or low-intensity sonication (50 W) and the hybridization of micrometer-sized GO sheets (Figure S2c, d in the Supporting Information) with PDDA-modified $SiO_2$ microspheres under intense sonication (160 W) were carried out as well. However, a number of GO linkages are found between the neighboring GO wrapped $SiO_2$ microspheres (Figure 2f−h), leading to their relatively poor water dispersity and causing the significant aggregation or sedimentation behaviors of their aqueous suspensions after setting overnight (Figure S5 in the Supporting Information). Accordingly, both continuously intense sonication and tiny sizes of GO sheets are crucial for prohibiting the common agglomeration phenomena during the hybridizations of GO with microspheric substrates, and are helpful for promoting the water dispersity of the resultant GO wrapped composite microspheres.

To functionalize the GO wrapped $SiO_2$ microspheres, we took advantage of the intrinsic reductivity of GO, which derived from its phenol-like moieties.[20] By heating treatment of an aqueous solution of $Ag(NH_3)_2OH$ in the presence of $SiO_2$@GO composite microspheres, numerous AgNPs were in situ synthesized on their surface because of the reducing effect of the outer GO layer toward such silver−ammonia complex, thereby yielding GO/AgNP composite film wrapped $SiO_2$ microspheres (denoted as $SiO_2$@GO@AgNPs) (see the Supporting Information for experimental details). Previous reports demonstrate that hydrazine is an effective reducing agent for the reduction of free GO sheets to RGO.[17,20,21] That is the same case for the immobilized GO sheets deposited on $SiO_2$@GO composite microspheres. As shown in Figure 3a, the aqueous suspension of $SiO_2$@GO composite microspheres gives an absorption band at 230 nm in its UV−vis spectrum (black curve), corresponding to $\pi \rightarrow \pi^*$ transition of aromatic C═C bonds in the immobilized GO sheets,[20−22] whereas it shifts to 260 nm (red curve) accompanied by the color transition of the aqueous suspension of $SiO_2$@GO composite microspheres from brown to black after heating treatment with hydrazine (Figure S6 in the Supporting Information). Such spectral change and color transition manifest that the deposited GO layer was reduced to RGO by hydrazine,[20−22] thus yielding RGO-wrapped $SiO_2$ microspheres (denoted as $SiO_2$@RGO). Therefore, chemical reduction of the GO component

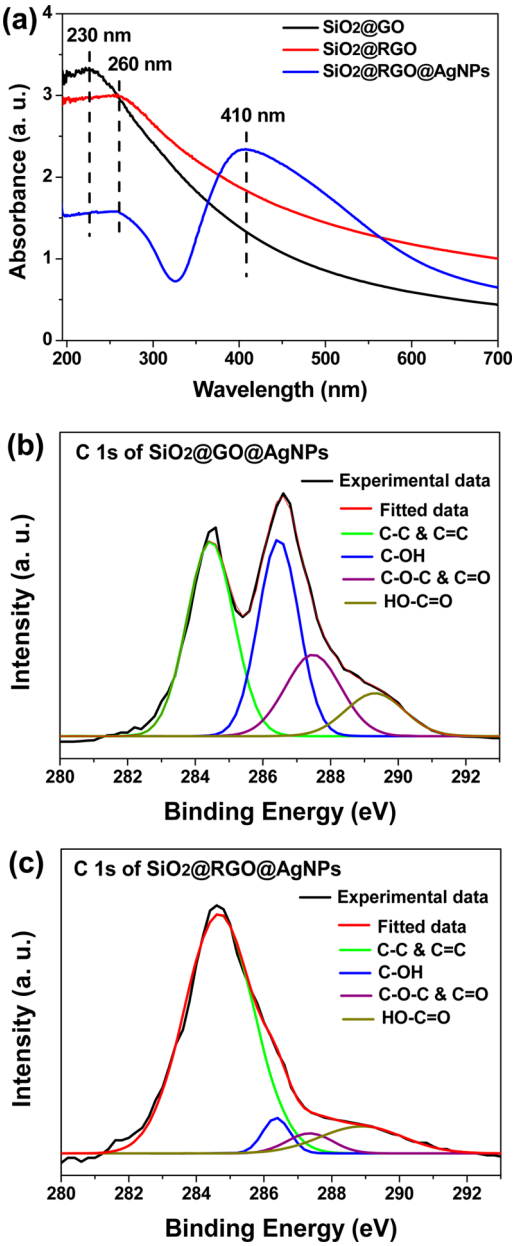


**Figure 3.** (a) UV−vis spectra of aqueous suspensions of $SiO_2$@GO (black curve), $SiO_2$@RGO (red curve), and $SiO_2$@RGO@AgNP (blue curve) composite microspheres. (b, c) High-resolution XPS spectra of C 1s regions of $SiO_2$@GO@AgNP and $SiO_2$@RGO@AgNP microspheres, respectively.

incorporated in $SiO_2$@GO@AgNP composite microspheres with hydrazine was performed to render RGO/AgNP composite film wrapped $SiO_2$ microspheres (denoted as $SiO_2$@RGO@AgNPs) (see the Supporting Information for experimental details). Figure 3b, c show the high-resolution X-ray photoelectron spectra (XPS) of C 1s regions of $SiO_2$@GO@AgNP and $SiO_2$@RGO@AgNP composite microspheres, respectively. The former demonstrates the abundance of various oxygen-containing functional groups of the GO component, like C−OH (286.5 eV), C−O−C (286.7 eV), C═O (286.7 eV) and HO−C═O (289.2 eV).[14,23] In sharp contrast, the latter shows that the oxygen-containing functional groups are efficiently removed from $SiO_2$@RGO@AgNP composite microspheres.[14,23] Consequently, the GO compo-


DOI: 10.1021/acsami.5b00296
ACS Appl. Mater. Interfaces 2015, 7, 6041−6046

nent within $SiO_2$@GO@AgNP composite was indeed reduced to RGO by hydrazine as well. In addition, the UV−vis spectrum of the aqueous dispersion of $SiO_2$@RGO@AgNP composite microspheres exhibits two absorption band (Figure 3a, blue curve). One is the RGO absorption band centered at 260 nm, and the other is located at 410 nm, which should arise from the surface plasmon resonance (SPR) absorption of the deposited AgNPs.[20,22] The high-resolution XPS spectrum of Ag 3d regions of $SiO_2$@RGO@AgNP composite microspheres (Figure S7 in the Supporting Information) reveals a representative curve for Ag 3d doublets with the binding energy of Ag $3d_{3/2}$ centered at 374 eV and the binding energy of Ag $3d_{5/2}$ centered at 368 eV. Such doublet splitting of 6 eV indicates the zero oxidation state of the deposited AgNPs.[22,24]

Figure 4 is a group of SEM and TEM images of $SiO_2$@RGO@AgNP microspheres, displaying a unique raspberrylike

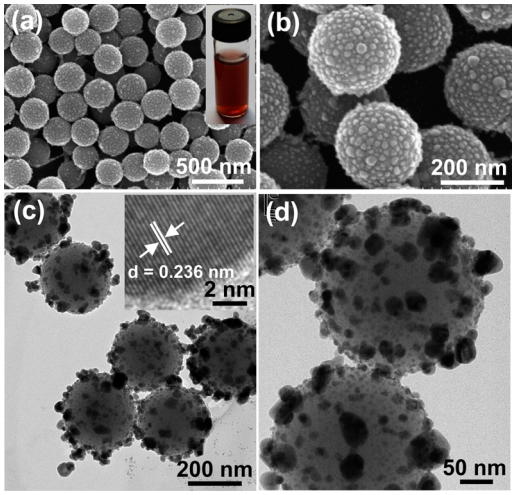


**Figure 4.** (a, b) SEM images of RGO/AgNP film wrapped $SiO_2$ microspheres (i.e., $SiO_2$@RGO@AgNP microspheres) at low and high magnifications, respectively; inset in a is the photograph of an aqueous suspension of $SiO_2$@RGO@AgNP microspheres after standing overnight, exhibiting the excellent water dispersity as well. (c, d) TEM images of $SiO_2$@RGO@AgNP microspheres at low and high magnifications, respectively; inset in c is the HRTEM image of an individual AgNP anchored a $SiO_2$@RGO@AgNP microsphere, showing its (111) lattice plane.

structure with lots of AgNPs well-distributed on their surface. As expected, the raspberrylike shape of $SiO_2$@RGO@AgNP microspheres is consistent with that of $SiO_2$@GO@AgNP microspheres (Figure S8 in the Supporting Information), implying that no significant morphological change took place after the hydrazine-involved reduction process. The diameters of the deposited AgNPs range from several nanometers to several tens of nanometers, and such polydisperse size distribution accounts for the broadness of their SPR absorption band as shown in Figure 3a (blue curve).[22,24] Inset of Figure 4c presents a HRTEM micrograph of an individual AgNP anchored on a $SiO_2$@RGO@AgNP microsphere, where the crystal lattice of the AgNP is clearly visible and the measured lattice fringe spacing of 0.236 nm corresponds to its (111) crystal plane.[20] Additionally, The Ag content in $SiO_2$@RGO@AgNP microspheres is 4% by weight as revealed by atomic absorption spectroscopic (AAS) measurement. Similar to $SiO_2$@GO composite microspheres, the dried $SiO_2$@RGO@AgNP microspheres can also be readily redispersed in water to form a homogeneous red suspension (inset of Figure 4a), which was so stable that no evident precipitate appeared after setting overnight, displaying highly water-dispersible performance. As control, the morphology and water dispersity of the RGO/AgNP film wrapped $SiO_2$ microspheres synthesized using micrometer-sized GO sheets were investigated as well. As shown in Figure S9 in the Supporting Information, cross-linkages remain to be observed between the neighboring composite microspheres, which contribute to the sedimentation behavior of their aqueous suspension to a large extent. These results once again demonstrate the importance of tiny GO sheets for the fabrication of highly water-dispersible GO- and RGO-based hybrid materials developed in the current system.

The catalytic activities of the surface-decorated $SiO_2$ microspheres were evaluated employing the reduction reaction of 4-nitrophenol (4-NP) by excessive amount of $NaBH_4$ and the process of which was monitored by UV−vis spectrometry (see the Supporting Information for experimental details). As shown in Figure S10 in the Supporting Information, the initial aqueous solution of 4-NP gives a characteristic peak centered at 317 nm, while it shifts to 400 nm upon addition of $NaBH_4$ owing to the formation of 4-nitrophenolate ions.[5,6] Because of the presence of kinetic barrier, this reduction reaction did not occur spontaneously without a necessary catalyst (Figure S10 in the Supporting Information).[5,22,25] By introducing $SiO_2$@RGO@AgNP or $SiO_2$@GO@AgNP microspheres to the reaction mixture, the peak at 400 nm dropped gradually as the reaction proceeded, and a new peak centered at 300 nm appeared (Figure 5a and Figure S11 in the Supporting Information), which was assigned to 4-aminophenol, the reduction product of 4-NP.[5,22,25] Figure 5b presents the plots of $\ln(A_t/A_0)$ as a function of time ($t$), where $A_0$ and $A_t$ correspond to the original absorbance of reaction mixture at 400 nm and its absorbance at 400 nm at time $t$, respectively. Linear correlation is commendably fitted in each case, indicating the pseudo-first order kinetics for the catalytic reduction reaction. According to the slopes of the fitted lines, the apparent rate constant $k$ can be directly determined to be 0.7 $min^{-1}$ for $SiO_2$@RGO@AgNP and 0.41 $min^{-1}$ $SiO_2$@GO@AgNP microspheres, respectively. While no catalytic activity was detected for the contrastive samples including pure $SiO_2$ microspheres, $SiO_2$ microspheres positively charged with PDDA as well as $SiO_2$@GO and $SiO_2$@RGO composite microspheres (Figure S12 in the Supporting Information), suggesting that the catalytic activities of the currently developed AgNP-containing composite microspheres mainly resulted from the deposited AgNPs. Moreover, the catalytic performance of the RGO/AgNP film wrapped $SiO_2$ microspheres synthesized using micrometer-sized GO sheets (denoted as $SiO_2$@$\mu$m-sized RGO@AgNPs) were also surveyed (Figure 5b and Figure S13 in the Supporting Information), and the corresponding apparent rate constant $k$ was determined to be 0.38 $min^{-1}$. Remarkably, compared with $SiO_2$@$\mu$m-sized RGO@AgNP microspheres, the $SiO_2$@RGO@AgNP microspheres exhibit preferable catalytic activity, which is likely due to their much better aqueous dispersity.

To compare the catalytic activities of the currently developed AgNP-containing composite microspheres with those of other AgNP-based hybrid catalysts, a parameter $k'$ is introduced, which is defined as the ratio of the apparent rate constant $k$ to the concentration of the added catalyst (i.e., $k' = k/c$). As a consequence, the $k'$ values for $SiO_2$@RGO@AgNP and $SiO_2$@GO@AgNP microspheres are 1400 and 820 $min^{-1}$ $mg^{-1}$ mL,


DOI: 10.1021/acsami.5b00296
ACS Appl. Mater. Interfaces 2015, 7, 6041−6046

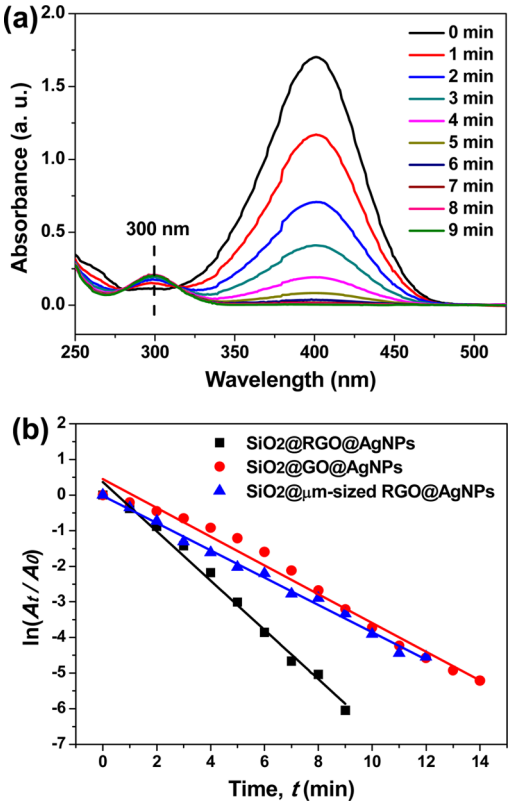


**Figure 5.** Catalytic performance of the currently developed AgNP-containing composite microspheres. (a) Successive UV−vis spectra of the reaction system for 4-NP reduction catalyzed by $SiO_2$@RGO@AgNP microspheres, which were recorded from the initiation of this catalytic reaction to its end at an interval of 1 min; the initial concentrations of the reaction mixture were 0.1 mM for 4-NP, 10 mM for $NaBH_4$ and 0.5 $\mu$g $mL^{-1}$ for $SiO_2$@RGO@AgNP microspheres. (b) Plots of $\ln(A_t/A_0)$ versus reaction time for catalytic reduction of 4-NP in the presence of $SiO_2$@RGO@AgNP microspheres (black square), $SiO_2$@GO@AgNP microspheres (red circle), and RGO/AgNP film wrapped $SiO_2$ microspheres synthesized using micrometer-sized GO sheets (denoted as $SiO_2$@$\mu$m-sized RGO@AgNPs) (blue triangle), respectively.

respectively. In previous reports, core−shell structured $Fe_3O_4$@C, titania, silica, and polymer microspheres have been employed as supports to anchor AgNPs and the corresponding $Fe_3O_4$@C@Ag, $TiO_2$@Ag, $SiO_2$@Ag, and polymer@Ag hybrid microspheres were fabricated and used for the catalytic reduction of 4-NP by $NaBH_4$.[24,26,27] However, none of the $k'$ values for these reported AgNP-based hybrid catalysts exceed 200 $min^{-1}$ $mg^{-1}$ mL in spite of their higher loading of AgNPs.[24,26,27] Hence, in terms of this point, the catalytic activities of the currently developed $SiO_2$@RGO@AgNP and $SiO_2$@GO@AgNP microspheres are much stronger and they feature more catalytic advantages. It is assumed that such superior catalytic activities of the currently developed $SiO_2$@RGO@AgNP and $SiO_2$@GO@AgNP microspheres are likely related to the incorporated RGO and GO components. Both RGO and GO possess charge mobility and provide $\pi-\pi$ stacking interaction with aromatic compounds.[28−30] As such, on one hand, the high affinity of the deposited RGO or GO component toward aromatic compounds enhances the adsorption of 4-NP on the surface of $SiO_2$@RGO@AgNP or $SiO_2$@GO@AgNP microspheres and thus increases the concentration of 4-NP near the metallic catalysts;[29,30] on the other hand, as reported in the previous literature, electron transfer from the deposited RGO or GO component to AgNPs increases the local electron concentration, facilitating the uptake of electrons by 4-NP molecules.[22,29,30] Obviously, both situations could dramatically accelerate the reduction reaction of 4-NP. Therefore, the synergistic effects between AgNPs and the incorporated RGO or GO component, together with the high water dispersity of $SiO_2$@RGO@AgNP and $SiO_2$@GO@AgNP microspheres, should be responsible for their outstanding catalytic performance. In addition, compared with GO, the $\pi$-electronic structure of RGO is more conjugated in nature, giving rise to its preferable electronic transport capability and $\pi-\pi$ stacking interaction with aromatic compounds.[28] Benefiting from these superior properties of RGO, the synergetic effect between AgNP and RGO components within $SiO_2$@RGO@AgNP microspheres should be better than that between the AgNP and GO components within $SiO_2$@GO@AgNP microspheres. That is the reason why $SiO_2$@RGO@AgNP microspheres exhibited relatively stronger catalytic activity than $SiO_2$@GO@AgNP microspheres (Figure 5b), despite their rather analogous structures and morphologies (Figure 4 and Figure S8 in the Supporting Information).

In summary, the common agglomeration problems generated during the hybridizations of GO or RGO sheets with functional microspheres have been effectively circumvented by adopting the currently developed methodology for sonication-assisted self-assembly of tiny GO sheets on microspheric substrates (e.g., PDDA-modified $SiO_2$ microspheres). Taking advantage of this facile strategy, we further fabricated highly water-dispersible RGO/AgNP film wrapped $SiO_2$ microspheres with unique raspberrylike morphology, which meanwhile showed extraordinary catalytic activity toward the reduction reaction of 4-nitrophenol by $NaBH_4$. Moreover, thanks to the convenience and versatility of the methodology presented in this work, it is believed that via sonication-assisted self-assembly of tiny GO sheets on other nonplanar supports with different constituents and morphologies, followed by functionalization with certain active species, more and more GO- and RGO-based hybrid materials with unique shape and reinforced properties will be developed and find applications in many practical and challenging fields such as catalysis, sensing, environmental protection, and so on.

## ■ ASSOCIATED CONTENT

### Supporting Information

Materials, experimental details, additional characterizations and the results of relevant control experiments. This material is available free of charge via the Internet at http://pubs.acs.org.

## ■ AUTHOR INFORMATION

### Corresponding Authors

*E-mail: showame@aliyun.com.
*E-mail: zyhcoco@163.com.

### Notes

The authors declare no competing financial interest.

## ■ ACKNOWLEDGMENTS

This work was supported by the National Natural Science Foundation of China (21401015, 21101136, and 21403020), the Basic and Frontier Research Program of Chongqing Municipality (cstc2014jcyjA50012, cstc2012jjA50037, and cstc2013jcyjA20023), the Natural Science Foundation of



DOI: 10.1021/acsami.5b00296
ACS Appl. Mater. Interfaces 2015, 7, 6041−6046

Yongchuan (Ycstc, 2014nc4001 and Ycstc, 2014nc3001), and the Foundation of Chongqing University of Arts and Sciences (R2013CJ04 and R2012CJ15).

## REFERENCES

(1) Novoselov, K. S.; Geim, A. K.; Morozov, S. V.; Jiang, D.; Zhang, Y.; Dubonos, S. V.; Grigorieva, I. V.; Firsov, A. A. Electric Field Effect in Atomically Thin Carbon Films. *Science* **2004**, *306*, 666−669.
(2) Lee, C.; Wei, X.; Kysar, J. W.; Hone, J. Measurement of the Elastic Properties and Intrinsic Strength of Monolayer Graphene. *Science* **2008**, *321*, 385−388.
(3) Yang, M.-Q.; Zhang, N.; Pagliaro, M.; Xu, Y.-J. Artificial Photosynthesis over Graphene−Semiconductor Composites. Are We Getting Better? *Chem. Soc. Rev.* **2014**, *43*, 8240−8254.
(4) Zhang, N.; Zhang, Y.; Xu, Y.-J. Recent Progress on Graphene-Based Photocatalysts: Current Status and Future Perspectives. *Nanoscale* **2012**, *4*, 5792−5813.
(5) Lu, W.; Ning, R.; Qin, X.; Zhang, Y.; Chang, G.; Liu, S.; Luo, Y.; Sun, X. Synthesis of Au Nanoparticles Decorated Graphene Oxide Nanosheets: Noncovalent Functionalization by TWEEN 20 in Situ Reduction of Aqueous Chloroaurate Ions for Hydrazine Detection and Catalytic Reduction of 4-Nitrophenol. *J. Hazard. Mater.* **2011**, *197*, 320−326.
(6) Zhang, Y.; Liu, S.; Lu, W.; Wang, L.; Tian, J.; Sun, X. In Situ Green Synthesis of Au Nanostructures on Graphene Oxide and Their Application for Catalytic Reduction of 4-Nitrophenol. *Catal. Sci. Technol.* **2011**, *1*, 1142−1144.
(7) Kim, H.-i.; Moon, G.-h.; Monllor-Satoca, D.; Park, Y.; Choi, W. Solar Photoconversion Using Graphene/$TiO_2$ Composites: Nanographene Shell on $TiO_2$ Core versus $TiO_2$ Nanoparticles on Graphene Sheet. *J. Phys. Chem. C* **2012**, *116*, 1535−1543.
(8) Kamat, P. V. Graphene-Based Nanoarchitectures. Anchoring Semiconductor and Metal Nanoparticles on a Two-Dimensional Carbon Support. *J. Phys. Chem. Lett.* **2010**, *1*, 520−527.
(9) Shao, J.-J.; Lv, W.; Yang, Q.-H. Self-Assembly of Graphene Oxide at Interfaces. *Adv. Mater.* **2014**, *26*, 5586−5612.
(10) Hwang, H.; Joo, P.; Kang, M. S.; Ahn, G.; Han, J. T.; Kim, B.-S.; Cho, J. H. Highly Tunable Charge Transport in Layer-by-Layer Assembled Graphene Transistors. *ACS Nano* **2012**, *6*, 2432−2440.
(11) Xi, Q.; Chen, X.; Evans, D. G.; Yang, W. Gold Nanoparticle-Embedded Porous Graphene Thin Films Fabricated via Layer-by-Layer Self-Assembly and Subsequent Thermal Annealing for Electrochemical Sensing. *Langmuir* **2012**, *28*, 9885−9892.
(12) Liu, J.; Tao, L.; Yang, W.; Li, D.; Boyer, C.; Wuhrer, R.; Braet, F.; Davis, T. P. Synthesis, Characterization, and Multilayer Assembly of pH Sensitive Graphene-Polymer Nanocomposites. *Langmuir* **2010**, *26*, 10068−10075.
(13) Lee, J. S.; You, K. H.; Park, C. B. Highly Photoactive, Low Bandgap $TiO_2$ Nanoparticles Wrapped by Graphene. *Adv. Mater.* **2012**, *24*, 1084−1088.
(14) Chen, Z.; Liu, S.; Yang, M.-Q.; Xu, Y.-J. Synthesis of Uniform CdS Nanospheres/Graphene Hybrid Nanocomposites and Their Application as Visible Light Photocatalyst for Selective Reduction of Nitro Organics in Water. *ACS Appl. Mater. Interfaces* **2013**, *5*, 4309−4319.
(15) Yang, S.; Feng, X.; Ivanovici, S.; Müllen, K. Fabrication of Graphene-Encapsulated Oxide Nanoparticles: Towards High-Performance Anode Materials for Lithium Storage. *Angew. Chem., Int. Ed.* **2010**, *49*, 8408−8411.
(16) Fan, W.; Zhang, C.; Tjiu, W. W.; Pramoda, K. P.; He, C.; Liu, T. Graphene-Wrapped Polyaniline Hollow Spheres as Novel Hybrid Electrode Materials for Supercapacitor Applications. *ACS Appl. Mater. Interfaces* **2013**, *5*, 3382−3391.
(17) Vickery, J. L.; Patil, A. J.; Mann, S. Fabrication of Graphene−Ploymer Nanocomposites with Higher-Order Three-Dimensional Architectures. *Adv. Mater.* **2009**, *21*, 2180−2184.
(18) Stöber, W.; Fink, A.; Bohn, E. Controlled Growth of Monodisperse Silica Spheres in the Micron Size Range. *J. Colloid Interface Sci.* **1968**, *26*, 62−69.
(19) Wang, W.; Gu, B.; Liang, L.; Hamilton, W. A. Fabrication of Two- and Three-Dimensional Silica Nanocolloidal Particle Arrays. *J. Phys. Chem. B* **2003**, *107*, 3400−3404.
(20) Pasricha, R.; Gupta, S.; Srivastava, A. K. A Facile and Novel Synthesis of Ag−Graphene-Based Nanocomposites. *Small* **2009**, *5*, 2253−2259.
(21) Fernández-Merino, M. J.; Guardia, L.; Paredes, J. I.; Villar-Rodil, S.; Solís-Fernández, P.; Martínez-Alonso, A.; Tascón, J. M. D. Vitamin C Is an Ideal Substitute for Hydrazine in the Reduction of Graphene Oxide Suspensions. *J. Phys. Chem. C* **2010**, *114*, 6426−6432.
(22) Zhang, Y.; Yuan, X.; Wang, Y.; Chen, Y. One-Pot Photochemical Synthesis of Graphene Composites Uniformly Deposited with Silver Nanoparticles and Their High Catalytic Activity towards the Reduction of 2-Nitroaniline. *J. Mater. Chem.* **2012**, *22*, 7245−7251.
(23) Feng, Y.; Feng, N.; Zhang, G.; Du, G. One-Pot Hydrothermal Synthesis of ZnS−Reduced Graphene Oxide Composites with Enhanced Photocatalytic Properties. *CrystEngComm* **2014**, *16*, 214−222.
(24) An, Q.; Yu, M.; Zhang, Y.; Ma, W.; Guo, J.; Wang, C. $Fe_3O_4$@Carbon Microspheres Supported Ag−Au Bimetallic Nanocrystals with the Enhanced Catalytic Activity and Selectivity for the Reduction of Nitroaromatic Compounds. *J. Phys. Chem. C* **2012**, *116*, 22432−22440.
(25) Chang, G.; Luo, Y.; Lu, W.; Qin, X.; Asiri, A. M.; Al-Youbi, A. O.; Sun, X. Ag Nanoparticles Decorated Polyaniline Nanofibers: Synthesis, Characterization, and Applications toward Catalytic Reduction of 4-Nitrophenol and Electrochemical Detection of $H_2O_2$ and Glucose. *Catal. Sci. Technol.* **2012**, *2*, 800−806.
(26) Zhu, M.; Wang, C.; Meng, D.; Diao, G. In Situ Synthesis of Silver Nanostructures on Magnetic $Fe_3O_4$@C Core−Shell Nanocomposites and Their Application in Catalytic Reduction Reactions. *J. Mater. Chem. A* **2013**, *1*, 2118−2125.
(27) Lu, Y.; Mei, Y.; Schrinner, M.; Ballauff, M.; Möller, M. W.; Breu, J. In Situ Formation of Ag Nanoparticles in Spherical Polyacrylic Acid Brushes by UV Irradiation. *J. Phys. Chem. C* **2007**, *111*, 7676−7681.
(28) Mkhoyan, K. A.; Contryman, A. W.; Silcox, J.; Stewart, D. A.; Eda, G.; Mattevi, C.; Miller, S.; Chhowalla, M. Atomic and Electronic Structure of Graphene-Oxide. *Nano Lett.* **2009**, *9*, 1058−1063.
(29) Luo, J.; Zhang, N.; Liu, R.; Liu, X. In Situ Green Synthesis of Au Nanoparticles onto Polydopamine-Functionalized Graphene for Catalytic Reduction of Nitrophenol. *RSC Adv.* **2014**, *4*, 64816−64824.
(30) Li, J.; Liu, C.-y.; Liu, Y. Au/Graphene Hydrogel: Synthesis, Characterization and Its Use for Catalytic Reduction of 4-Nitrophenol. *J. Mater. Chem.* **2012**, *22*, 8426−8430.


DOI: 10.1021/acsami.5b00296
*ACS Appl. Mater. Interfaces* 2015, 7, 6041−6046